ARTICLE OPEN ACCESS

Association of Early β-Amyloid Accumulation and Neuroinflammation Measured With [^{11}C] PBR28 in Elderly Individuals Without Dementia

Sini Toppala, MD, Laura L. Ekblad, MD, PhD, Jouni Tuisku, MSc, Semi Helin, MSc, Jarkko J. Johansson, PhD, Hanna Laine, MD, PhD, Eliisa Löyttyniemi, MSc, Päivi Marjamäki, PhD, Kaj Blennow, MD, PhD, Henrik Zetterberg, MD, PhD, Antti Jula, MD, PhD, Matti Viitanen, MD, PhD, and Juha O. Rinne, MD, PhD

Correspondence
Dr. Toppala
sini.toppala@utu.fi

Neurology® 2021;96:e1608-e1619. doi:10.1212/WNL.0000000000011612

Abstract

Objective

To examine whether early β–amyloid (Aβ) accumulation and metabolic risk factors are associated with neuroinflammation in elderly individuals without dementia.

Methods

We examined 54 volunteers (mean age 70.0 years, 56% women, 51% *APOE* ε4 carriers) with the translocator protein (TSPO) tracer [^{11}C]PBR28 to assess neuroinflammation and with [^{11}C] Pittsburgh compound B (PiB) to assess cerebral Aβ accumulation. [^{11}C]PBR28 and [^{11}C]PiB standardized uptake value ratios (SUVRs) were quantified in 6 regions of interests by using the cerebellar cortex as a pseudo-reference and reference region, respectively. Fasting venous glucose, insulin, and high-sensitivity C-reactive protein (hs-CRP) values were determined. Homeostatic model assessment of insulin resistance (HOMA-IR) was calculated. A subset of individuals (n = 11) underwent CSF sampling, and $A\beta_{40}$, $A\beta_{42}$, total tau, phospho-tau, soluble TREM2, and YKL-40 levels were measured.

Results

Among the whole study group, no significant association was found between [^{11}C]PiB and [^{11}C] PBR28 SUVR composite scores (slope 0.02, $p = 0.30$). However, higher [^{11}C]PiB binding was associated with higher [^{11}C]PBR28 binding among amyloid-negative ([^{11}C]PiB composite score ≤1.5) (TSPO genotype–, age- and sex-adjusted slope 0.26, $p = 0.008$) but not among amyloid-positive (slope −0.004, $p = 0.88$) participants. Higher CSF soluble TREM2 ($r_s = 0.72$, $p = 0.01$) and YKL-40 ($r_s = 0.63$, $p = 0.04$) concentrations were associated with a higher [^{11}C]PBR28 composite score. Higher body mass index, HOMA-IR, and hs-CRP were associated with higher [^{11}C]PBR28 binding in brain regions where Aβ accumulation is first detected in Alzheimer disease.

Conclusions

While there was no association between amyloid and neuroinflammation in the overall study group, neuroinflammation was associated with amyloid among the subgroup at early stages of amyloid pathology.

From the Turku PET Centre (S.T., L.L.E., J.T., S.H., J.J., P.M., J.O.R.) and Department of Biostatistics (E.L.), University of Turku; Kuopio City Home Care (S.T.), Rehabilitation and Medical Services for Elderly, Kuopio, Finland; Amsterdam Alzheimer Center (L.L.E.), Amsterdam UMC, the Netherlands; Department of Radiation Sciences (J.J.), Umeå University, Sweden; City of Turku (H.L.), Welfare Division, Turku City Hospital, Turku, Finland; Department of Medicine (H.L.), University of Turku, Turku University Hospital, Finland; Department of Psychiatry and Neurochemistry (K.B., H.Z.), Institute of Neuroscience and Physiology, the Sahlgrenska Academy at the University of Gothenburg; Clinical Neurochemistry Laboratory (K.B., H.Z.), Sahlgrenska University Hospital, Mölndal, Sweden; Department of Neurodegenerative Disease (H.Z.), UCL Institute of Neurology, Queen Square; UK Dementia Research Institute at UCL (H.Z.), London; National Institute for Health and Welfare (A.J.); Department of Geriatrics (M.V.), Turku City Hospital; University of Turku (M.V.), Finland; Division of Clinical Geriatrics (M.V.), NVS, Karolinska Institutet, Stockholm, Sweden; and Division of Clinical Neurosciences (J.O.R.), Turku University Hospital, Finland.

Go to Neurology.org/N for full disclosures. Funding information and disclosures deemed relevant by the authors, if any, are provided at the end of the article.

The Article Processing Charge was funded by FinELib.

Glossary

Aβ = amyloid-β; **AD** = Alzheimer disease; **BMI** = body mass index; **DVR** = distribution volume ratio; **HAB** = high-affinity binder; **HOMA-IR** = homeostatic model assessment of insulin resistance; **hs-CRP** = high-sensitivity C-reactive protein; **MAB** = mixed-affinity binder; **MCI** = mild cognitive impairment; **P-tau** = phosphorylated tau; **PiB** = Pittsburgh compound B; **ROI** = region of interest; **sTREM2** = soluble TREM2; **SUV** = standardized uptake value; **SUVR** = SUV ratio; **T-tau** = total tau; **TSPO** = translocator protein.

Neuroinflammation, that is, activation of microglia and astrocytes, seems to play an important role in the pathogenesis of Alzheimer disease (AD) and other diseases leading to dementia.[1,2] Metabolic risk factors, including obesity and insulin resistance, have been linked to cognitive decline and dementia.[3–5] However, little is known about the possible relationship among chronic low-grade inflammation, metabolic risk factors, neuroinflammation, and the neuropathology of AD.

Activated microglia overexpress 18-kDa translocator protein (TSPO), and thus PET imaging with tracers binding to TSPO is used to assess neuroinflammation.[6,7] TREM2 is an innate immune receptor that is selectively expressed by microglia in the CNS. Its soluble variant (sTREM2)[8] and YKL-40, a glycoprotein expressed by reactive astrocytes and microglia in the CNS, can be measured from the CSF.[9] Studies have suggested that both of these markers of neuroinflammation are increased in the early stage of AD.[8,10,11]

On the basis of previous literature,[12,13] we hypothesized that increased TSPO expression would associate with amyloid-β (Aβ) accumulation in the cerebral cortex and that both TSPO expression and Aβ accumulation would associate with CSF biomarkers of neuroinflammation and AD. Previous reports have shown that midlife metabolic risk factors predict brain Aβ accumulation[14,15] and dementia.[16,17] Therefore, we hypothesized that insulin resistance, obesity, and chronic low-grade inflammation measured by high-sensitivity C-reactive protein (hs-CRP) would associate with increased neuroinflammation.

To test these hypotheses, we examined 54 elderly volunteers without dementia with brain PET imaging using a TSPO radioligand [^{11}C]PBR28 and Aβ radioligand [^{11}C] Pittsburgh compound B (PiB). In addition, we performed CSF analyses on a subset of the study population.

Methods

The study participants took part in a neuroimaging study carried out at the Turku PET Centre in 2014 to 2016. The study was conducted to investigate the associations among midlife insulin resistance, inflammation, and late-life brain Aβ accumulation, neuroinflammation, cerebrovascular lesions, and cognition. The results concerning Aβ accumulation, cognitive performance, and cerebrovascular lesions have been published previously.[15,18] The study participants were recruited from a nationwide Finnish health examination survey, the Health 2000 survey, according to their insulin sensitivity and *APOE* genotype in 2000. The recruitment process has been described in detail previously.[15,18]

Health 2000 Survey

The Health 2000 survey is a Finnish nationwide, population-based study carried out in 2000 to 2001 and conducted by the Finnish Institute for Health and Welfare. Eight thousand twenty-eight individuals >30 years of age were randomly selected from the Finnish population register. Six thousand three hundred fifty-four volunteers (79% participation rate, mean age 55.4 years) attended the health examination proper. A thorough physical examination was performed; body mass index (BMI) was determined; and venous blood samples, including fasting insulin and glucose, and hs-CRP were drawn.[19,20] *APOE* genotype was defined with the MassARRAY System (Sequenom, San Diego, CA) with a modified protocol.[21] Homeostatic model assessment of insulin resistance (HOMA-IR) was calculated with the equation fasting insulin (μU/mL) times fasting glucose (mmol/L) divided by 22.5.[22]

Study Participants and Recruitment Process in 2014

In 2014, we recruited 60 participants from those who had attended the Health 2000 survey to attend further examination at the Turku PET Center according to their HOMA-IR values in 2000 and their *APOE* genotype. All participants were community-dwelling individuals who did not require help with their activities of daily living. We recruited 30 participants who had insulin resistance in 2000 (IR+ group, HOMA-IR in the highest tertile [>2.17] of the Health 2000 study population) and 30 controls with normal insulin sensitivity (IR− group, HOMA-IR in the lowest tertile [<1.25] of the Health 2000 study population). Both groups were enriched for *APOE* ε4 carriers to obtain 15 *APOE* ε4 carriers in both groups. On the basis of a telephone interview, individuals with a history of a major stroke, a previous dementia diagnosis, any other major neurologic disorder, type 2 diabetes in 2000, and type 2 diabetes after the year 2000 for the insulin-sensitive group were excluded. Additional exclusion criteria were any contraindication for a PET or MRI scan.

The participants' genotypes for TSPO binding were determined before [^{11}C]PBR28 imaging because of the large interindividual variability in the binding affinity of [^{11}C]PBR28 due to the rs6971 polymorphism of the TSPO gene.[23] TSPO genotyping was performed in London, UK (Imperial Molecular Pathology Laboratory, Hammersmith Hospital).

DNA was extracted from peripheral blood with the Qiagen (Venlo, the Netherlands) QIAamp DNA blood mini kit. TSPO genotyping was performed with a TaqMan Allelic Discrimination assay. Among the 60 participants, there were 5 low-affinity binders. They all were excluded from the present study, leaving 55 eligible participants. In addition, 1 individual was excluded because of not being able to finish the 70 minutes of [^{11}C]PBR28 scanning.

Standard Protocol Approvals, Registrations, and Patient Consents

The Finnish Health 2000 study was approved by the Ethics Committee for Epidemiology and Public Health in the hospital district of Helsinki and Uusimaa, Finland. The follow-up study was approved by the Ethics Committee of the Hospital District of Southwest Finland. Written informed consent was obtained from all of the participants. Separate written consent for CSF sampling was obtained from all participants who agreed to undergo a lumbar puncture. All study procedures were conducted according to Good Clinical Practice guidelines and the Declaration of Helsinki.

Laboratory Examination at Time of PET Scans in 2014 to 2016

The laboratory examinations were performed within 4 months of the [^{11}C]PBR28 scan. Venous blood samples were drawn after an overnight fasting (minimum 10 hours) in 2014 to 2016. Serum insulin and glucose were determined as previously described.[18] HOMA-IR was calculated.[22] hs-CRP was determined by immunonephelometry with a BN ProSpec System (Siemens Healthcare GmbH, Marburg, Germany).

A subset of 11 participants gave permission to obtain CSF samples. The samples were centrifuged within 30 minutes and stored at −70°C. The samples were sent to the University of Gothenburg for further analysis. CSF YKL-40 concentration was measured with an YKL-40 ELISA kit (R&D Systems, Minneapolis, MN). CSF $A\beta_{40}$ and $A\beta_{42}$ concentrations were measured with electrochemiluminescence technology and the MS6000 Human Abeta 3-Plex Ultra-Sensitive Kit (Meso Scale Discovery, Rockville, MD). CSF total tau (T-tau) and phosphorylated tau (P-tau) concentrations were measured with commercially available INNOTEST sandwich ELISAs (Fujirebio Europe, Ghent, Belgium). CSF sTREM2 concentration was measured with an in-house ELISA as previously described.[24] All CSF biomarker measurements were performed with 1 batch of reagents in 1 round of experiments by board-certified laboratory technicians who were blinded to clinical data. Intra-assay coefficients of variation of quality control samples were <10%.

MRI and PET Scanning With TSPO Radioligand [^{11}C]PBR28 and [^{11}C]PiB

To obtain anatomic reference and to be able to exclude potential structural abnormalities, the study volunteers underwent MRI with a 3T PET-MRI scanner (Philips Ingenuity TF PET-MR device, Philips Healthcare, Best, the Netherlands).

[^{11}C]PBR28 PET imaging was performed to assess microglial activation, and [^{11}C]PiB PET imaging was done to assess Aβ accumulation in the brain. Both the dynamic 70-minute [^{11}C]PBR28 PET and the dynamic 90-minute [^{11}C]PiB PET scans were performed with a brain-dedicated high-resolution PET scanner, the ECAT HRRT (Siemens Medical Solutions, Knoxville, TN). An individually shaped thermoplastic mask was used to minimize head movement.

[^{11}C]PBR28 was manufactured as previously reported.[25] An anesthesiologist performed arterial catheterization before imaging for those who did not have any contraindication (anticoagulant therapy) for arterial cannulation (n = 44). The participants received the [^{11}C]PBR28 as a rapid intravenous bolus (mean dose 496 MBq, SD 19 MBq). Arterial blood samples measuring radioactivity and metabolites were collected. The additional details of [^{11}C]PBR28 PET data acquisition, reconstruction, arterial blood sampling, and radiometabolite analysis have been presented previously.[25] The [^{11}C]PiB PET scanning protocol was described earlier.[15]

PET images were realigned and coregistered to individual T1-weighted MRIs with SPM12 software (Wellcome Trust Centre for Neuroimaging, London, UK) running in MATLAB (MathWorks, Natick, MA). Automated region of interest (ROI) generation was conducted for both [^{11}C]PBR28 and [^{11}C]PiB data with FreeSurfer software (version 5.3.0, freesurfer.net/) and T1-weighted MRI data as input. Six ROIs were formed (parietal cortex, prefrontal cortex, anterior cingulum, posterior cingulum, precuneus, lateral temporal cortex) based on regions where Aβ accumulation typically begins in AD.[26] (Specific FreeSurfer regions [all bilateral]: parietal cortex: inferior parietal, superior parietal, and supramarginal cortex; prefrontal cortex: caudal middle frontal, lateral orbitofrontal, medial orbitofrontal, pars opercularis, pars orbitalis, pars triangularis, rostral middle frontal, and frontal pole cortex; anterior cingulum: caudal anterior cingulate, and rostral anterior cingulate cortex; posterior cingulum: isthmus cingulate, and posterior cingulate cortex; precuneus: precuneus cortex; lateral temporal cortex: inferior temporal, middle temporal, superior temporal, temporal pole, and transverse temporal cortex.)

For the analysis of regional and voxel-by-voxel [^{11}C]PBR28 (n = 54) data, we used a standardized uptake value (SUV) ratio (SUVR) from 30 to 70 minutes with respect to cerebellum pseudoreference region, which has been validated previously.[27] In addition, distribution volume (V_T) was calculated for those with arterial blood data (n = 44) using Logan analysis within a 30- to 70-minute interval, after which distribution volume ratios (DVRs) were calculated by dividing the target ROI V_T by the cerebellar cortex V_T. We used a 2-sample *t* test to ensure that the SUVs and V_T values of the cerebellar cortex did not differ between the amyloid-negative and amyloid-positive groups. Regional and voxel-by-voxel [^{11}C]PiB SUVs were calculated using imaging data from 60 to 90 minutes after the tracer injection. SUVRs were obtained with the cerebellar cortex used as a reference region.

Table 1 Study Population Characteristics According to Amyloid Positivity

	Amyloid Negative (PiB SUVR ≤1.5) (n = 29)	Amyloid Positive (PiB SUVR >1.5) (n = 25)	*p* Value
Age, mean (SD), y	69.8 (3.8)	70.2 (2.4)	0.59
Women, n (%)	16 (55)	15 (60)	0.72
***APOE* ε4 genotype, n (%)**	6 (20.7)	21 (84)	<0.0001
BMI, mean (SD), kg/m^2	26.5 (4.2)	26.7 (3.8)	0.87
Hb_{A1c}, median (Q1, Q3), mmol/mol	36 (34–39)	34 (32–35)	0.19
Fasting glucose, median (Q1, Q3), mmol/L	5.7 (5.4–6.1)	5.5 (5.3–6.2)	0.85
Fasting insulin, median (Q1, Q3), mU/L	9 (6.5–12)	10 (6.5–16)	0.11
HOMA-IR, median (Q1, Q3)	2.3 (1.6–3.1)	3.0 (1.5–4.5)	0.17
hs-CRP, median (Q1, Q3), mg/L	1.1 (0.5–2.8)	1.1 (0.7–1.8)	0.80
Serum total cholesterol, mean (SD), mmol/L	5.0 (1.1)	5.1 (0.8)	0.79
CERAD total score, median (Q1, Q3)	91 (87–95)	85 (72–93)	0.06
[^{11}C]PiB SUVR composite score, median (Q1, Q3)	1.31 (1.27–1.37)	1.84 (1.64–2.27)	<0.0001
TSPO genotype MAB, n (%)	12 (41)	13 (52)	0.44
TSPO genotype HAB, n (%)	17 (59)	12 (48)	0.44
[^{11}C]PBR28 SUVR composite score, median (Q1, Q3)	1.06 (1.04–1.11)	1.08 (1.05–1.15)	0.08

Abbreviations: BMI = body mass index; CERAD = Consortium to Establish a Registry for Alzheimer's Disease; HAB = high-affinity binder; Hb_{A1c} = glycated hemoglobin; HOMA-IR = homeostatic model assessment of insulin resistance; hs-CRP = high-sensitivity C-reactive protein; MAB = mixed-affinity binder; PiB = Pittsburgh compound B; Q1, Q3 = interquartile range; SUVR = standardized uptake value ratio; TSPO = translocator protein.
[^{11}C]PiB -PET scan was considered amyloid positive when [^{11}C]PiB SUVR composite score was >1.5. Composite [^{11}C]PBR28 and [^{11}C]PiB SUVR scores were calculated as the average SUVR over all 6 regions of interest. The *p* values for differences between amyloid-negative and amyloid-positive individuals were assessed with the Student *t* test or Wilcoxon rank-sums test (CERAD total score and [^{11}C]PiB SUVR composite score) for continuous variables and with Pearson χ^2 test for categorical variables. A logarithmic transformation is used for Hb_{A1c}, fasting glucose, fasting insulin, HOMA-IR, and hs-CRP to achieve normal distribution.

Composite cortical [^{11}C]PBR28 and [^{11}C]PiB SUVR scores were calculated as a volume-weighted average [^{11}C]PBR28 SUVR and [^{11}C]PiB SUVR over all 6 ROIs. The [^{11}C]PiB-PET scan was considered amyloid positive when the [^{11}C]PiB composite SUVR score was >1.5 according to previous studies on cognitively healthy elderly populations.[28,29]

Statistical Analyses

The associations between explanatory variables ([^{11}C]PiB SUVRs/BMI/HOMA-IR/hs-CRP) and [^{11}C]PBR28 SUVR composite score, [^{11}C]PBR28 SUVRs of the 6 cortical ROIs, and [^{11}C]PBR28 DVRs of the same ROIs (n = 44) were studied with multivariable linear models. The explanatory variables were adjusted for age, sex, and TSPO genotype because previous studies have shown that they can affect [^{11}C]PBR28 binding[23,25,30] and that SUVR levels might be paradoxically lower in high-affinity binders (HABs) than mixed-affinity binders (MABs) for TSPO genotype.[27] To achieve a normal distribution, a logarithmic transformation was performed for HOMA-IR and hs-CRP. Normality assumption for the analyses was checked from the residuals. Bonferroni correction for multiple comparisons was performed for the analyses of individuals ROIs (uncorrected *p* values were multiplied by the number of ROIs studied, i.e., 6).

The association between the CSF proteins and [^{11}C]PiB and [^{11}C]PBR28 SUVR composite scores was assessed with nonparametric Spearman correlation because the parameters were not normally distributed.

Two-sided statistical significance was set at $p < 0.05$. The statistical analyses were performed with SAS JMP Pro 14 (SAS Institute, Cary, NC). Voxel-by-voxel associations between [^{11}C]PBR28 SUVRs and [^{11}C]PiB SUVRs were assessed with SPM12 by using normalized SUVR images in Montreal Neurological Institute space. The images were smoothed with 3-dimensional gaussian 8-mm full width at half-maximum filter to ensure normality before the statistical analysis.

Data Availability

Anonymized data are available on reasonable request for a study that has been approved by a local ethics committee.

Results

Demographics

The characteristics of the study population according to amyloid status are shown in table 1. The mean age of the

Table 2 Study Population Characteristics in 2014 to 2016 in the Subset of Individuals With CSF Data (n = 11)

Age, mean (SD), y	68.1 (2.2)
Women, n (%)	6 (54.5)
***APOE* ε4 genotype, n (%)**	5 (45.5)
BMI, mean (SD), kg/m^2	26.1 (3.5)
Hb_{A1c}, median (Q1, Q3), mmol/mol	34 (33–34)
Fasting glucose, median (Q1, Q3), mmol/L	5.6 (5.3–5.9)
Fasting insulin, median (Q1, Q3), mU/L	9 (4–12)
HOMA-IR, median (Q1, Q3)	2.32 (0.98–3.15)
hs-CRP, median (Q1, Q3), mg/L	0.8 (0.6–2.6)
Serum total cholesterol, mean (SD), mmol/L	5.7 (0.73)
CERAD total score, median (Q1, Q3)	94 (85–95)
[^{11}C]PiB SUVR composite score, median (Q1, Q3)	1.37 (1.30–1.58)
Amyloid positive, n (%)	3 (27.3)
TSPO binding genotype MAB, n (%)	5 (45.5)
TSPO binding genotype HAB, n (%)	6 (54.5)
[^{11}C]PBR28 SUVR composite score, median (Q1, Q3)	1.05 (1.02–1.12)
$Aβ_{40}$, median (Q1, Q3), pg/mL	7,798 (5,627–8,355)
$Aβ_{42}$, median (Q1, Q3), pg/mL	633.4 (475.5–1048.2)
Tau, median (Q1, Q3), pg/mL	233.0 (202.3–323.3)
Phosphorylated tau, median (Q1, Q3), pg/mL	40.8 (33.6–53.8)
YKL-40, median (Q1, Q3), ng/mL	133 (111–155)
sTREM2, median (Q1, Q3), pg/mL	3,647 (3,370–4,502)

Abbreviations: Aβ = β-amyloid; BMI = body mass index; CERAD = Consortium to Establish a Registry for Alzheimer's Disease; HAB = high-affinity binder; Hb_{A1c} = glycated hemoglobin; HOMA-IR = homeostatic model assessment of insulin resistance; hs-CRP = high-sensitivity C-reactive protein; MAB = mixed-affinity binder; PiB = Pittsburgh compound B; Q1, Q3 = interquartile range; sTREM2 = soluble TREM2; SUVR = standardized uptake value ratio; TSPO = translocator protein.
[^{11}C]PiB -PET scan was considered amyloid positive when [^{11}C]PiB SUVR composite score was >1.5. Composite [^{11}C]PBR28 and [^{11}C]PiB SUVR scores were calculated as the average SUVR over all 6 ROIs.

participants was 70.0 years (range 65–80 years). The average BMI was 26.6 kg/m^2 (range 19.7–38.8 kg/m^2). There were 25 MABs and 29 HABs. Twenty-five participants (46%) were amyloid positive. There were no differences between amyloid-negative and amyloid-positive participants in age, sex, BMI, fasting glucose, hs-CRP, or total cholesterol. Amyloid-positive individuals were more often *APOE* ε4 carriers. Amyloid-positive participants tended to have a lower Consortium to Establish a Registry for Alzheimer's Disease total score, as expected, but this difference was not statistically significant (p = 0.06). One individual (amyloid positive, MAB) had exceptionally high [^{11}C]PBR28 SUVR values in all ROIs ([^{11}C]PBR28 SUVR composite score 1.40) and an exceptionally high BMI (38.8 kg/m^2) and HOMA-IR value (21.4) among the study population. This outlier was excluded from all analyses.

CSF samples were obtained from 11 individuals (mean age 68.1 years), of which 6 were women. There were 5 MABs and 6 HABs. Five individuals (46%) were *APOEε4* carriers. The mean BMI was 26.1 kg/m^2. Only 3 of the participants who underwent CSF sampling were classified as amyloid positive (table 2).

Higher [^{11}C]PBR28 Binding Associated With Higher [^{11}C]PiB Binding in Amyloid-Negative Participants

Among all participants (amyloid negative and amyloid positive), no significant association was found between [^{11}C]PiB and [^{11}C]PBR28 SUVR composite scores (slope 0.02, p = 0.30) or between [^{11}C]PiB SUVRs and [^{11}C]PBR28 SUVRs in any of the ROIs (all $p \geq 0.21$) (data not shown).

To evaluate whether the association between [^{11}C]PiB and [^{11}C]PBR28 SUVR composite scores would be modulated by amyloid status based on [^{11}C]PiB PET scans, we analyzed the interaction of [^{11}C]PiB composite score × amyloid positivity for predicting [^{11}C]PBR28 SUVR composite score. TSPO genotype was added into the analysis as an explanatory variable. The interaction for [^{11}C]PiB composite score × amyloid positivity was statistically significant (p = 0.02); thus, the analyses were stratified according to amyloid positivity.

A higher [^{11}C]PiB SUVR composite score was associated with a higher [^{11}C]PBR28 SUVR composite score among amyloid-negative participants (slope 0.26, p = 0.008). Among amyloid-positive participants, no association between [^{11}C]PiB and [^{11}C]PBR28 SUVR composite scores was found (slope −0.004, p = 0.88) (figure 1).

Voxel Level Analysis of the Association Between [^{11}C]PiB and [^{11}C]PBR28 Binding

To evaluate the association between [^{11}C]PiB and [^{11}C]PBR28 without predefined assumptions of specific ROIs, we performed voxel-level analysis on 53 participants (outlier excluded). TSPO genotype was added as an explanatory variable in the analyses. Among amyloid-negative participants, [^{11}C]PiB binding showed a positive association with [^{11}C]PBR28 binding, especially in the parietal cortex, but also in the frontal cortex, in the precuneus, and in the posterior cingulum, reflecting cortical regions of early Aβ accumulation in AD (figure 1, false discovery rate–corrected p < 0.05). A positive association was found between [^{11}C]PiB and [^{11}C]PBR28 in the false discovery rate–corrected voxel-level analysis in the entire study population as well (data not shown). However, the association was explained by the amyloid-negative subgroup; no association was found between [^{11}C]PiB and [^{11}C]PBR28 for the amyloid-positive participants.

Figure 1 Association Between [^{11}C]PiB and [^{11}C]PBR28 Binding

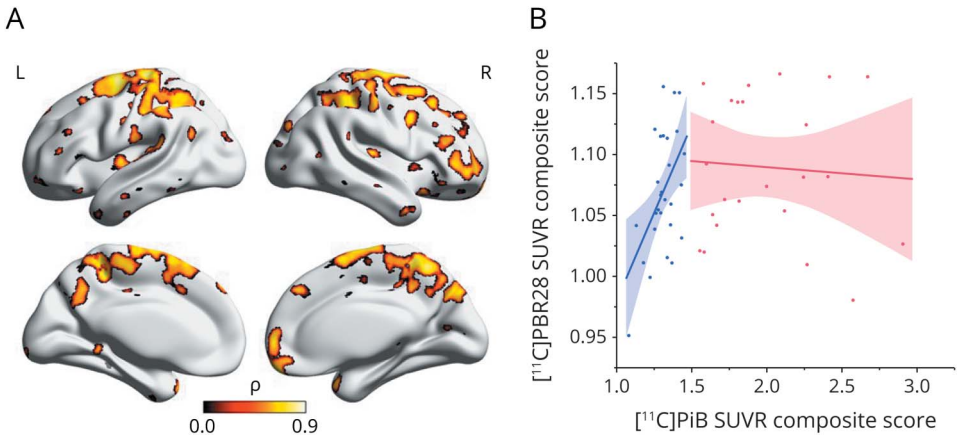

(A) Voxel-level analysis showing statistically significant partial correlation coefficients (ρ) between higher [^{11}C] Pittsburgh compound B (PiB) uptake and higher [^{11}C]PBR28 uptake among amyloid-negative participants. Subcortical regions were excluded from the analysis, and translocator protein (TSPO) genotype was used as a control variable. Correction for multiple comparisons was carried out with false discovery rate with a significance level of $p < 0.05$. (B) Association between [^{11}C]PiB standardized uptake value ratio (SUVR) composite score and [^{11}C] PBR28 SUVR composite score. Amyloid-negative participants are marked with blue and amyloid positive participants with red.

CSF sTREM2 and YKL-40 Associated With [^{11}C] PBR28, and CSF $A\beta_{42}$ and $A\beta42/A\beta_{40}$ Ratio Associated With [^{11}C]PiB

We used the CSF results to support our results from the PET scans by measuring proteins related to AD and inflammation and evaluating the correlation between CSF proteins and [^{11}C]PiB and [^{11}C]PBR28 binding. The results of the CSF analysis are presented in table 2. All the participants had T-tau and P-tau levels within the normal range.

A higher CSF sTREM2 value and a higher CSF YKL-40 value was associated with a higher [^{11}C]PBR28 SUVR composite score (figure 2 and table 3). A lower CSF $A\beta_{42}$ level and a lower CSF $A\beta_{42}/A\beta_{40}$ ratio, but not $A\beta_{40}$, were associated with a higher [^{11}C]PiB SUVR composite score (table 3).

Metabolic Risk Factors Measured at Time of PET Scans in 2014 to 2016 Associated With [^{11}C] PBR28

A higher BMI was associated with a higher [^{11}C]PBR28 SUVR composite score ($p = 0.006$). A positive association between BMI and [^{11}C]PBR28 SUVR was found in the parietal cortex (Bonferroni corrected $p < 0.0006$) and in the precuneus (Bonferroni-corrected $p = 0.002$). In other ROIs, no significant association between BMI and [^{11}C]PBR28 SUVRs was found (all uncorrected $p \geq 0.10$) (table 4 and figure 3).

HOMA-IR or hs-CRP did not associate with [^{11}C]PBR28 composite score (HOMA-IR $p = 0.21$, hs-CRP $p = 0.29$). The associations between HOMA-IR and hs-CRP and [^{11}C] PBR28 SUVRs are shown in table 4. The association between

Figure 2 Association Between CSF (A) sTREM2 and (B) YKL-40 Concentration and [^{11}C]PBR28 SUVR Composite Score

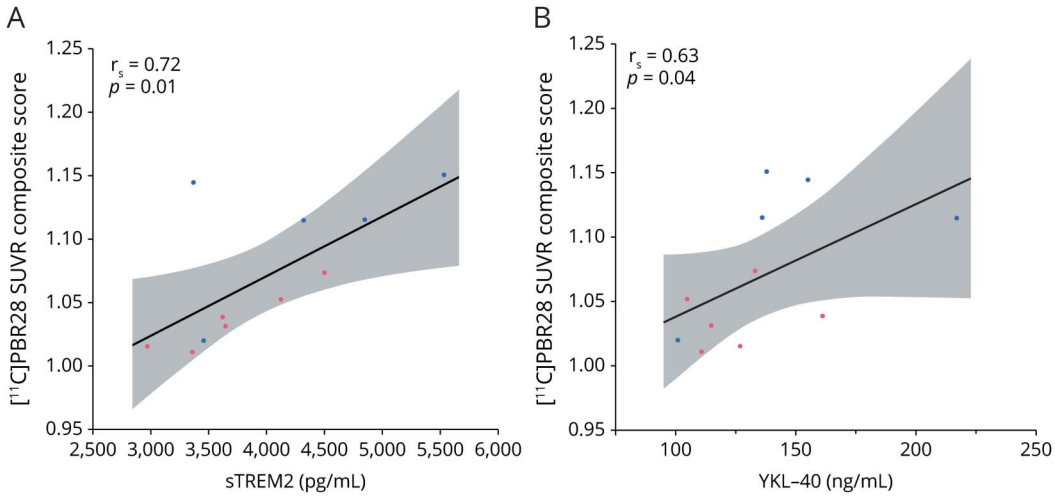

[^{11}C]PBR28 standardized uptake value ratio (SUVR) composite score is calculated as the average SUVR over 6 regions of interest. High-affinity binders are marked with red dots; mixed-affinity binders are marked with blue dots.

Table 3 Associations Between CSF Biomarkers and [^{11}C]PBR28 SUVR Composite Score and Between CSF Biomarkers and [^{11}C]PiB SUVR Composite Score (n = 11) Assessed With Spearman Correlation

	[^{11}C]PBR28 SUVR Composite Score		[^{11}C]PiB SUVR Composite Score	
CSF biomarker	**r_s Value**	***p* Value**	**r_s Value**	***p* Value**
YKL-40	0.63	0.04	−0.31	0.36
sTREM2	0.72	0.01	−0.06	0.85
$A\beta_{40}$	0.69	0.02	−0.27	0.42
$A\beta_{42}$	0.12	0.73	−0.85	0.001
$A\beta_{42}/A\beta_{40}$ ratio	−0.26	0.43	−0.87	0.0005
Total tau	0.47	0.14	−0.21	0.54
Phosphorylated tau	0.59	0.06	−0.34	0.31

Abbreviation: Aβ = β-amyloid; PiB = Pittsburgh compound B; sTREM2 = soluble TREM2; SUVR = standardized uptake value ratio.

HOMA-IR and [^{11}C]PBR28 SUVR in the parietal cortex remained significant even after Bonferroni correction (Bonferroni-corrected $p = 0.005$) (table 4 and figure 3).

Additional analyses were performed with [^{11}C]PBR28 DVRs based on the arterial data instead of SUVRs (n = 44). The results were almost similar to those obtained with SUVRs. BMI was associated with [^{11}C]PBR28 DVR composite score ($p = 0.03$). Significant associations were found between BMI and [^{11}C]PBR28 DVR in the parietal cortex ($p < 0.0006$) and the precuneus ($p = 0.049$) and between hs-CRP and [^{11}C]PBR28 DVR in the parietal cortex ($p = 0.03$) after Bonferroni correction (data not shown).

A Higher BMI in Midlife Predicted Microglial Activation Measured by [^{11}C]PBR28 PET Imaging 15 Years Later

To evaluate whether midlife risk factors would associate with late-life neuroinflammation, we analyzed the associations between metabolic variables measured in 2000 and [^{11}C]PBR28 SUVRs measured in 2014 to 2016. A higher BMI in midlife associated with a higher [^{11}C]PBR28 SUVR in the parietal cortex (uncorrected $p = 0.002$) and precuneus (uncorrected $p = 0.03$). Only the association between BMI and [^{11}C]PBR28 SUVR in parietal cortex was significant after Bonferroni correction (Bonferroni-corrected $p = 0.01$). Neither baseline HOMA-IR nor hs-CRP associated with [^{11}C]PBR28 SUVRs in any of the ROIs (all uncorrected $p \geq 0.07$). As expected, there was a strong correlation between midlife and late-life BMI ($r = 0.77$, $p < 0.0001$) (data not shown).

Discussion

Contrary to our original hypothesis, no association was seen between amyloid and neuroinflammation among the whole study group. However, we found that neuroinflammation might be associated with the early stages of Aβ accumulation in elderly individuals without dementia. The association between [^{11}C]PiB and [^{11}C]PBR28 SUVR composite scores was seen among amyloid-negative participants only. In addition, higher levels of metabolic risk factors (BMI, HOMA-IR, and hs-CRP) were positively associated with neuroinflammation measured with [^{11}C]PBR28 PET in brain regions where Aβ accumulation is first detected in AD. The results are supported by the finding that CSF sTREM2 and YKL-40, 2 previously established markers for neuroinflammation, were positively associated with our main outcome, the [^{11}C]PBR28 SUVR composite score.

To date, few studies have used second-generation TSPO ligands to assess the relationship between neuroinflammation and AD. Most of the previous studies evaluating the role of neuroinflammation in the AD pathologic process have been performed with a traditional TSPO ligand, [^{11}C](R)PK11195. It has been suggested that [^{11}C](R)PK11195 has limited sensitivity and specificity,[31] whereas second-generation TSPO ligands might have higher specific TSPO binding.[32] However, no head-to-head study has compared [^{11}C]PBR28 and [^{11}C](R)PK11195 PET in AD, and thus, there is no convincing evidence suggesting that one ligand would be more sensitive than the other.[7] A recent meta-analysis of 28 PET studies (of which 4 had been performed with [^{11}C]PBR28) indicated that patients with AD have increased TSPO levels compared to healthy controls especially within frontotemporal regions.[33] According to one of the studies included in the meta-analysis, [^{11}C]PBR28 binding was higher in cortical brain regions among patients with AD compared to controls, but there was no difference between patients with mild cognitive impairment (MCI) and controls.[34] However, another study showed higher [^{11}C]PBR28 uptake in amyloid-positive patients with MCI compared to healthy controls.[35] In a longitudinal study (mean follow-up time 2.7 years), patients with AD had a greater increase in TSPO binding in temporoparietal regions than controls.[36] Studies focusing on neuroinflammation in elderly individuals at risk for AD are scarce.

Table 4 Association Between Metabolic Variables Measured in 2014 to 2016 at Time of PET Scans and [^{11}C]PBR28 SUVRs

ROI	Prefrontal cortex	Parietal cortex	Lateral temporal cortex	Precuneus	Anterior cingulum	Posterior cingulum	Composite score
Age-, sex-, and TSPO genotype–adjusted slope (95% CI)							
BMI	0.0035 (−0.00067 to 0.0077)	0.011[c,e] (0.0066 to 0.014)	0.00034 (−0.0030 to 0.0037)	0.0094[c,d] (0.0044 to 0.014)	−0.0009 (−0.0063 to 0.0044)	0.0033 (−0.0013 to 0.0079)	0.0048[b] (0.00152 to 0.0082)
HOMA-IR	0.0017 (−0.020 to 0.024)	0.040[c,d] (0.017–0.062	−0.0043 (−0.021 to 0.013)	0.030[a] (0.0020 to 0.058)	−0.035[b] (−0.060 to −0.0090)	−0.0043 (−0.028 to 0.020)	0.011 (−0.068 to 0.030)
hs-CRP	0.00022 (−0.015 to 0.016)	0.022[a] (0.0054 to 0.039)	0.0015 (−0.011 to 0.014)	0.0094 (−0.011 to 0.030)	−0.0054 (−0.025 to 0.014)	−0.0045 (−0.022 to 0.012)	0.0069 (−0.0061 to 0.020)

Abbreviations: BMI = body mass index; HOMA-IR = homeostatic model assessment of insulin resistance; hs-CRP = high-sensitivity C-reactive protein; ROI = region of interest; SUVR = standardized uptake value ratio; TSPO = translocator protein.
Results are shown as slope (95% confidence interval). Associations between BMI and [^{11}C]PBR28 SUVR, HOMA-IR, and [^{11}C]PBR28 SUVR and hs-CRP and [^{11}C]PBR28 SUVR are analyzed in separate linear models. [^{11}C]PBR28 SUVR composite score is calculated as the average [^{11}C]PBR28 SUVR over all 6 ROIs. A logarithmic transformation is used for HOMA-IR and hs-CRP to achieve normal distribution.
[a]$p < 0.05$, [b]$p < 0.01$, [c]$p < 0.001$. Bonferroni-corrected p values (uncorrected p values * 6, correction performed for single ROI analyses, but not for the analyses concerning the [^{11}C]PBR28 composite score). [d]$p < 0.01$, [e]$p < 0.001$.

Neuroinflammation is assumed to be both beneficial and detrimental, depending on the stage of AD pathogenesis.[7] Presumably, the initial microglial activation would be protective, but it would become unfavorable with disease progression.[37,38] A [^{11}C]PBR28 study demonstrated that there could be 2 microglial activation peaks in the AD pathogenesis: an early protective peak and a later proinflammatory peak.[13] In line with previous TSPO-PET studies,[2,7] our results suggest that neuroinflammation occurs at early stages of the AD pathogenesis. A previous [^{11}C]PBR28 study found a correlation between Aβ load measured with [^{18}F]flutemetamol and [^{11}C]PBR28 binding.[12] The correlation was stronger among patients with MCI than patients with AD.[12] A TSPO-PET study with [^{18}F]DPA-714 found an increase of TSPO binding in patients with AD, especially at the prodromal stage, compared to controls.[38] In addition, they found higher TSPO binding in slow decliners than in fast decliners, with no difference in Aβ accumulation, indicating that microglial activation might have a protective role.[38] However, in a longitudinal study, the same study group showed that the subsequent increase in [^{18}F]DPA-714 binding among patients with AD was associated with disease worsening.[39] In the present study, we found an association between Aβ accumulation and [^{11}C]PBR28 among amyloid-negative participants but not among amyloid-positive participants, suggesting that neuroinflammation might be associated with early stages of Aβ accumulation.

Contrary to a previous study that found higher TSPO binding (measured with ^{18}F-DPA-714) among amyloid-positive controls compared to amyloid-negative controls,[38] we did

Figure 3 Associations Between Metabolic Variables and [^{11}C]PBR28 Binding in the Parietal Cortex

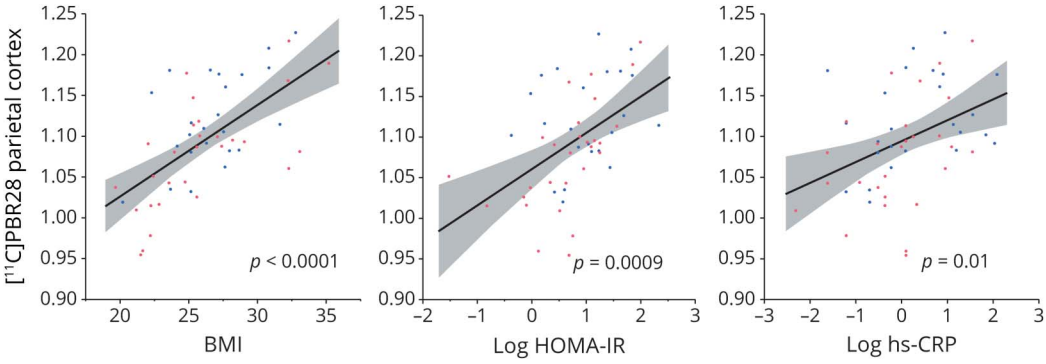

Logarithmic transformation is used for homeostatic model assessment of insulin resistance (HOMA-IR) and high-sensitivity C-reactive protein (hs-CRP). [^{11}C]PBR28 binding is reported as standardized uptake value ratio. High-affinity binders are marked with red dots; mixed-affinity binders are marked with blue dots. Age-, sex-, and translocator protein genotype–adjusted p values for the association between body mass index (BMI; kg/m^2) and [^{11}C]PBR28, HOMA-IR and [^{11}C]PBR28, and hs-CRP and [^{11}C]PBR28 were assessed with multivariable linear models, uncorrected for multiple comparisons.

not find any group difference in microglial activation between amyloid-negative and amyloid-positive participants. However, the control groups in the previous study (6 amyloid-positive and 20 amyloid-negative controls) were smaller than our study groups, and the quantification was performed without arterial blood samples.

We found that higher CSF sTREM2 and YKL-40 levels were associated with higher [^{11}C]PBR28 binding in the cerebral cortex. According to a meta-analysis, CSF sTREM2 and YKL-40 levels are higher in both patients with MCI and patients with AD compared to healthy controls.[40] Another meta-analysis showed that CSF YKL-40 is associated with clinically diagnosed AD, but the relationship seems to be notably weaker than that of the core biomarkers $A\beta_{42}$, T-tau, and P-tau.[41] To date, the association between CSF markers of neuroinflammation and TSPO binding in PET imaging has been studied insufficiently. A study investigating neuroinflammation in treated HIV-positive individuals did not find any associations between CSF chemokines and [^{11}C]PBR28 binding.[42] Our finding of a positive association between CSF sTREM2 and YKL-40 levels and [^{11}C]PBR28 SUVRs strengthens the assumption that the [^{11}C]PBR28 SUVRs might serve as a measurement of neuroinflammation.

We found that metabolic risk factors (higher BMI and insulin resistance) and low-grade inflammation (hs-CRP) associated positively with [^{11}C]PBR28 SUVR in brain regions where Aβ accumulation is first detected in AD, although the results concerning hs-CRP did not survive correction for multiple comparisons. Our findings are supported by epidemiologic studies showing that chronic low-grade inflammation,[43,44] obesity,[16] and insulin resistance[3–5] are associated with cognitive decline. It has been suggested that environmentally modifiable risk factors of cognitive decline such as chronic inflammation and obesity would affect the risk through a sustained neuroinflammatory drive.[1] Epidemiologic studies have suggested a link between nonsteroidal anti-inflammatory drugs and reduced risk of clinically diagnosed AD.[45,46] However, most of the randomized controlled trials assessing the use of nonsteroidal anti-inflammatory drugs in AD treatment have yielded negative results; thus, they are not recommended for the prevention of AD.[47] We have previously shown that midlife insulin resistance predicts Aβ accumulation in the brain,[15] and midlife obesity has been shown to independently predict late-life brain Aβ accumulation.[14] In the present study, no association was found between midlife insulin resistance or low-grade inflammation and neuroinflammation, possibly reflecting that neuroinflammation is a dynamic process whereas brain Aβ accumulation presumably begins decades before the onset of the first symptoms of AD. Our study suggests that the association between metabolic risk factors and neuroinflammation is seen in brain regions where Aβ is first accumulated in AD. However, our results concerning metabolic risk factors are to be considered preliminary and warrant further investigation. Contrary to our findings regarding the association between BMI and [^{11}C]PBR28 binding, a multicenter study on healthy controls from our center and 2 other centers found a negative correlation between BMI and [^{11}C]PBR28 V_T values in gray matter, thalamus, and hippocampus by using arterial plasma curves as an input function in kinetic modeling.[25] Most likely, these contrasting results are emerging because, in the present study, a cerebellar gray matter pseudoreference region was used as a model input instead of plasma input function. The previous study focused on [^{11}C]PBR28 binding in healthy controls across different age groups, while the present study focused on neuroinflammation that would be related to AD pathology. Because AD pathologic changes are rarely seen in the cerebellar cortex, we used the cerebellar cortex as a pseudoreference region in the analyses, consistent with previous reports on AD.[27,36]

Our study had limitations. TSPO quantification by PET is challenging partly because of the large interindividual variability in the binding affinity of [^{11}C]PBR28 due to the rs6971 polymorphism.[23] In addition, there is no true reference region in the brain for [^{11}C]PBR28 imaging. TSPO expression is seen throughout the brain and blood vessels; there is no brain region totally devoid of specific TSPO binding sites.[27] Traditionally, analysis of [^{11}C]PBR28 PET binding requires arterial blood sampling. However, a study group has previously validated an SUVR method in [^{11}C]PBR28-PET imaging in patients with AD.[27] The cerebellum is used as a pseudoreference region in the method[27] on the basis of the findings that the cerebellar cortex is typically devoid of neuropathologic changes typical for AD, including inflammation.[48,49] The study group also confirmed that cerebellar SUVs did not differ between patients with AD and MCI and controls. Furthermore, the SUVR method may have greater sensitivity compared to the gold standard method in which V_T is calculated from the 2-tissue-compartment model with the arterial input function.[27] We did not have arterial blood sampling data on all participants, which can be considered a limitation. However, we performed our analyses both with the SUVR method (n = 54) using cerebellum as a pseudoreference region and with the DVR method using the arterial data (n = 44). Both analysis methods yielded similar results, confirming previous reports that SUVR can be used to detect cortical [^{11}C]PBR28 binding to detect AD-related neuroinflammation.[27,36] We did not perform partial volume corrections, but the partial volume effect was minimized by the use of a high-resolution PET scanner. Moreover, the participants in our study did not have dementia or significant brain atrophy. Nevertheless, lack of partial volume correction could be regarded as a limitation. According to a recent postmortem study, TSPO is expressed not only in microglia but also in astrocytes, endothelial cells, and vascular smooth muscle cells.[50] Thus, PBR28 binding can be influenced by other cell types than microglia. The main advantage of this study is the possibility of combining [^{11}C]PBR28 and [^{11}C]PiB PET results in elderly individuals without dementia. A strength is that we used the CSF results to support our results from the PET scans, even if the CSF samples were obtained from 11 participants only, which limits firm conclusions based on the CSF results. Additional benefits are the arterial blood sampling in [^{11}C]PBR28 PET imaging from the majority of the study

population and the long follow-up time (15 years) in terms of the metabolic risk factors.

While neuroinflammation was not associated with amyloid among all participants, this study suggests that neuroinflammation may be associated with the early stages of brain Aβ pathology. We also demonstrate that metabolic risk factors (higher BMI, insulin resistance, and chronic low-grade inflammation) are associated with neuroinflammation in brain regions where Aβ accumulation is first detected in AD. We propose that the association between metabolic risk factors and clinically diagnosed AD seen in epidemiologic studies could be mediated at least partly through neuroinflammation. It should be noted, however, that the early stages of Aβ accumulation in elderly individuals with normal cognition might not lead to symptomatic AD. Larger studies with longitudinal protocols are needed to understand the complex relationship between metabolic risk factors, neuroinflammation, brain Aβ accumulation, and AD and particularly to detect the time course of neuroinflammation in the pathogenesis of AD. Our ongoing follow-up study on the same study population will provide insights into the longitudinal associations among neuroinflammation, amyloid accumulation, and cognitive performance. Future studies combining CSF analyses with TSPO imaging and amyloid and tau-PET imaging could provide new targets to develop novel therapies for AD.

Acknowledgment

The authors thank all the study volunteers for their contribution.

Study Funding

This study was funded by Finnish Governmental Research Funding (ERVA) for Turku University Hospital and Turku City Hospital, the Pro Humanitate Foundation, the Finnish Cultural Foundation, the Sigrid Juselius Foundation, and the Päivikki and Sakari Sohlberg Foundation.

Disclosure

S. Toppala received personal grants from the Betania Foundation, the Uulo Arhio Foundation, the Finnish Medical Foundation, the Juho Vainio Foundation, and the Turku University Foundation and personal fees from Finnish Governmental Research Funding (ERVA). L.L. Ekblad received personal grants from the Finnish Medical Foundation, Turunmaan Duodecim Foundation, the Paulo Foundation, and the Sigrid Juselius Foundation and personal fees from Finnish Governmental Research Funding (ERVA). J. Tuisku is supported by the Alfred Kordelin Foundation, the Instrumentarium Science Foundation, the Orion Research Foundation, the Paulo Foundation, the Päivikki and Sakari Sohlberg Foundation, and Turku University Hospital Foundation. S Helin, J. Johansson, H. Laine, E. Löyttyniemi, and P. Marjamäki report no disclosures. K. Blennow is supported by the Swedish Research Council (No. 2017-00915), the Alzheimer Drug Discovery Foundation, USA (No. RDAPB-201809-2016615), the Swedish Alzheimer Foundation (No. AF-742881), Hjärnfonden, Sweden (No. FO2017-0243), the Swedish state under the agreement between the Swedish government and the county councils, the ALF agreement (No. ALFGBG-715986), and European Union Joint Program for Neurodegenerative Disorders (JPND2019-466-236). K. Blennow has served as a consultant or at advisory boards for Abcam, Axon, Biogen, Lilly, MagQu, Novartis, and Roche Diagnostics and is a cofounder of Brain Biomarker Solutions in Gothenburg AB, a GU Venture–based platform company at the University of Gothenburg. H. Zetterberg is a Wallenberg Scholar supported by grants from the Swedish Research Council (No. 2018-02532), the European Research Council (No. 681712), Swedish State Support for Clinical Research (No. ALFGBG-720931), the Alzheimer Drug Discovery Foundation, USA (No. 201809-2016862), and the UK Dementia Research Institute at UCL. H. Zetterberg has served at scientific advisory boards for Denali, Roche Diagnostics, Wave, Samumed, and CogRx; has given lectures in symposia sponsored by Fujirebio, Alzecure, and Biogen; and is a cofounder of Brain Biomarker Solutions in Gothenburg AB, a GU Ventures–based platform company at the University of Gothenburg. A. Jula and M. Viitanen report no disclosures. J.O. Rinne has received research grants from the Sigrid Juselius Foundation, Finnish State Research Funding, and Academy of Finland (grant 310962). He serves as a neurology consultant for CRST (Clinical Research Services Turku) Oy. Go to Neurology.org/N for full disclosures.

Publication History

Received by *Neurology* April 30, 2020. Accepted in final form December 10, 2020.

Appendix Authors

Name	Location	Contribution
Sini Toppala, MD	Turku PET Centre, University of Turku, Finland; Kuopio City Home Care, Rehabilitation and Medical Services for Elderly, Finland	Analysis and interpretation of data, performed the statistical analyses, and wrote the manuscript
Laura Ekblad, MD, PhD	Turku PET Centre, University of Turku, Finland; Amsterdam Alzheimer Center, Amsterdam UMC, the Netherlands	Study concept and design, acquisition of data, interpretation of data, and drafted and revised the manuscript for intellectual content
Jouni Tuisku, MSc	Turku PET Centre, University of Turku, Finland	Reconstructed the [^{11}C]PBR28 PET images, performed the quantitative analysis of the imaging data, and drafted and revised the manuscript for intellectual content
Semi Helin, MSc	Turku PET Centre, University of Turku, Finland	Manufactured [^{11}C]PBR28 and [^{11}C]PIB, and drafted and revised the manuscript for intellectual content

Continued

Appendix *(continued)*

Name	Location	Contribution
Jarkko Johansson, PhD	Turku PET Centre, University of Turku, Finland; Department of Radiation Sciences, Umeå University, Sweden	Reconstructed the [^{11}C]PIB PET images, performed the quantitative analysis of the imaging data, and drafted and revised the manuscript for intellectual content
Hanna Laine, MD, PhD	Turku City Hospital, University of Turku, Finland; Department of Medicine, University of Turku, Turku University Hospital, Finland	Study concept and design, drafted and revised the manuscript for intellectual content
Eliisa Löyttyniemi, MSc	Department of Biostatistics, University of Turku, Finland	Guided the statistical analyses, and drafted and revised the manuscript for intellectual content
Päivi Marjamäki, PhD	Turku PET Centre, University of Turku, Finland	Performed the [^{11}C]PBR28 metabolite analysis, and drafted and revised the manuscript for intellectual content
Kaj Blennow, MD, PhD	Department of Psychiatry and Neurochemistry, Institute of Neuroscience and Physiology, the Sahlgrenska Academy at the University of Gothenburg, Mölndal, Sweden; Clinical Neurochemistry Laboratory, Sahlgrenska University Hospital, Mölndal, Sweden	Was in charge of the CSF analyses, and drafted and revised the manuscript for intellectual content
Henrik Zetterberg, MD, PhD	Department of Psychiatry and Neurochemistry, Institute of Neuroscience and Physiology, the Sahlgrenska Academy at the University of Gothenburg, Mölndal, Sweden; Clinical Neurochemistry Laboratory, Sahlgrenska University Hospital, Mölndal, Sweden; Department of Neurodegenerative Disease, UCL Institute of Neurology, Queen Square, London, UK; UK Dementia Research Institute at UCL, London	Was in charge of the CSF analyses, and drafted and revised the manuscript for intellectual content
Antti Jula MD, PhD	National Institute for Health and Welfare, Turku, Finland	Study concept and design, interpretation of data, and drafted and revised the manuscript for intellectual content
Matti Viitanen MD, PhD	Turku City Hospital, University of Turku, Finland; Clinical Geriatrics, Karolinska Institutet, Karolinska University Hospital, Huddinge, Sweden	Study concept and design, interpretation of data, and drafted and revised the manuscript for intellectual content
Juha O. Rinne, MD, PhD	Turku PET Centre, University of Turku, Finland; Division of Clinical Neurosciences, Turku University Hospital, Finland	Study concept and design, interpretation of data, and drafted and revised the manuscript for intellectual content

References

1. Heneka MT, Carson MJ, El Khoury J, et al. Neuroinflammation in Alzheimer's disease. Lancet Neurol 2015;14:388–405.
2. Calsolaro V, Edison P. Neuroinflammation in Alzheimer's disease: current evidence and future directions. Alzheimers Dement 2016;12:719–732.
3. Whitmer RA, Gustafson DR, Barrett-Connor E, Haan MN, Gunderson EP, Yaffe K. Central obesity and increased risk of dementia more than three decades later. Neurology 2008;71:1057–1064.
4. Schrijvers EMC, Witteman JCM, Sijbrands EJG, Hofman A, Koudstaal PJ, Breteler MMB. Insulin metabolism and the risk of Alzheimer disease: the Rotterdam study. Neurology 2010;75:1982–1987.
5. Ekblad LL, Rinne JO, Puukka P, et al. Insulin resistance predicts cognitive decline: an 11-year follow-up of a nationally representative adult population sample. Diabetes Care 2017;40:751–758.
6. Schain M, Kreisl WC. Neuroinflammation in neurodegenerative disorders: a review. Curr Neurol Neurosci Rep 2017;17:25.
7. Edison P, Brooks DJ. Role of neuroinflammation in the trajectory of Alzheimer's disease and in vivo quantification using PET. J Alzheimers Dis 2018;64(suppl 1): S339–S351.
8. Suárez-Calvet M, Kleinberger G, Araque Caballero MÁ, et al. sTREM2 cerebrospinal fluid levels are a potential biomarker for microglia activity in early-stage Alzheimer's disease and associate with neuronal injury markers. EMBO Mol Med 2016;8:466–476.
9. Cantó E, Tintoré M, Villar LM, et al. Chitinase 3-like 1: prognostic biomarker in clinically isolated syndromes. Brain 2015;138:918–931.
10. Nordengen K, Kirsebom BE, Henjum K, et al. Glial activation and inflammation along the Alzheimer's disease continuum. J Neuroinflammation 2019;16:46.
11. Janelidze S, Mattsson N, Stomrud E, et al. CSF biomarkers of neuroinflammation and cerebrovascular dysfunction in early Alzheimer disease. Neurology 2018;91: e867–e877.
12. Dani M, Wood M, Mizoguchi R, et al. Microglial activation correlates in vivo with both tau and amyloid in Alzheimer's disease. Brain 2018;141:2740–2754.
13. Fan Z, Brooks DJ, Okello A, Edison P. An early and late peak in microglial activation in Alzheimer's disease trajectory. Brain 2017;140:792–803.
14. Gottesman RF, Schneider ALC, Zhou Y, et al. Association between midlife vascular risk factors and estimated brain amyloid deposition. JAMA 2017;317:1443–1450.
15. Ekblad LL, Johansson J, Helin S, et al. Midlife insulin resistance, APOE genotype, and late-life brain amyloid accumulation. Neurology 2018;90:e1150–e1157.
16. Kivipelto M, Ngandu T, Fratiglioni L, et al. Obesity and vascular risk factors at midlife and the risk of dementia and Alzheimer disease. Arch Neurol 2005;62:1556–1560.
17. Kivimäki M, Luukkonen R, Batty GD, et al. Body mass index and risk of dementia: analysis of individual-level data from 1.3 million individuals. Alzheimers Dement 2018;14:601–609.
18. Toppala S, Ekblad LL, Lötjönen J, et al. Midlife insulin resistance as a predictor for late-life cognitive function and cerebrovascular lesions. J Alzheimers Dis 2019;72: 215–228.
19. Heistaro S Methodology Report: Health 2000 Survey[online]. Helsinki: National Public Health Institute; 2008;B26. Available at julkari.fi/handle/10024/78185. Accessed January 3, 2020.
20. Aromaa A, Koskinen S. Health and functional capacity in Finland. Baseline Results of the Health 2000 Health Examination Survey [online]. Helsinki: National Public Health Institute; 2004;B12. Available at julkari.fi/handle/10024/78534. Accessed January 3, 2020.
21. Jänis MT, Siggins S, Tahvanainen E, et al. Active and low-active forms of serum phospholipid transfer protein in a normal Finnish population sample. J Lipid Res 2004;45:2303–2309.
22. Matthews DR, Hosker JP, Rudenski AS, Naylor BA, Treacher DF, Turner RC. Homeostasis model assessment: insulin resistance and beta-cell function from fasting plasma glucose and insulin concentrations in man. Diabetologia 1985;28:412–419.
23. Owen DR, Yeo AJ, Gunn RN, et al. An 18-kDa translocator protein (TSPO) polymorphism explains differences in binding affinity of the PET radioligand PBR28. J Cereb Blood Flow Metab 2012;32:1–5.
24. Gisslén M, Heslegrave A, Veleva E, et al. CSF concentrations of soluble TREM2 as a marker of microglial activation in HIV-1 infection. Neurol Neuroimmunol Neuroinflamm 2019;6:e512.
25. Tuisku J, Plavén-Sigray P, Gaiser EC, et al. Effects of age, BMI and sex on the glial cell marker TSPO: a multicentre [11C]PBR28 HRRT PET study. Eur J Nucl Med Mol Imaging 2019;46:2329–2338.
26. Braak H, Braak E. Frequency of stages of Alzheimer-related lesions in different age categories. Neurobiol Aging 1997;18:351–357.
27. Lyoo CH, Ikawa M, Liow JS, et al. Cerebellum can serve as a pseudo-reference region in Alzheimer disease to detect neuroinflammation measured with PET radioligand binding to translocator protein. J Nucl Med 2015;56:701–706.
28. Jack CR, Lowe VJ, Senjem ML, et al. 11C PiB and structural MRI provide complementary information in imaging of Alzheimer's disease and amnestic mild cognitive impairment. Brain 2008;131:665–680.
29. Rowe CC, Ellis KA, Rimajova M, et al. Amyloid imaging results from the Australian Imaging, Biomarkers and Lifestyle (AIBL) study of aging. Neurobiol Aging 2010;31: 1275–1283.
30. Kreisl WC, Jenko KJ, Hines CS, et al. A genetic polymorphism for translocator protein 18 kDa affects both in vitro and in vivo radioligand binding in human brain to this putative biomarker of neuroinflammation. J Cereb Blood Flow Metab 2013;33:53–58.
31. Ching ASC, Kuhnast B, Damont A, Roeda D, Tavitian B, Dollé F. Current paradigm of the 18-kDa translocator protein (TSPO) as a molecular target for PET imaging in

neuroinflammation and neurodegenerative diseases. Insights Imaging 2012;3:111–119.
32. Fujita M, Kobayashi M, Ikawa M, et al. Comparison of four 11C-labeled PET ligands to quantify translocator protein 18 kDa (TSPO) in human brain: (R)-PK11195, PBR28, DPA-713, and ER176: based on recent publications that measured specific-to-non-displaceable ratios. EJNMMI Res 2017;7:84.
33. Bradburn S, Murgatroyd C, Ray N. Neuroinflammation in mild cognitive impairment and Alzheimer's disease: a meta-analysis. Ageing Res Rev 2019;50:1–8.
34. Kreisl WC, Lyoo CH, McGwier M, et al. In vivo radioligand binding to translocator protein correlates with severity of Alzheimer's disease. Brain 2013;136:2228–2238.
35. Fan Z, Dani M, Femminella GD, et al. Parametric mapping using spectral analysis for 11C-PBR28 PET reveals neuroinflammation in mild cognitive impairment subjects. Eur J Nucl Med Mol Imaging 2018;45:1432–1441.
36. Kreisl WC, Lyoo CH, Liow JS, et al. 11C-PBR28 binding to translocator protein increases with progression of Alzheimer's disease. Neurobiol Aging 2016;44:53–61.
37. Van Eldik LJ, Carrillo MC, Cole PE, et al. The roles of inflammation and immune mechanisms in Alzheimer's disease. Alzheimers Dement 2016;2:99–109.
38. Hamelin L, Lagarde J, Dorothée G, et al. Early and protective microglial activation in Alzheimer's disease: a prospective study using 18F-DPA-714 PET imaging. Brain 2016;139:1252–1264.
39. Hamelin L, Lagarde J, Dorothée G, et al. Distinct dynamic profiles of microglial activation are associated with progression of Alzheimer's disease. Brain 2018;141:1855–1870.
40. Shen XN, Niu LD, Wang YJ, et al. Inflammatory markers in Alzheimer's disease and mild cognitive impairment: a meta-analysis and systematic review of 170 studies. J Neurol Neurosurg Psychiatry 2019;90:590–598.
41. Olsson B, Lautner R, Andreasson U, et al. CSF and blood biomarkers for the diagnosis of Alzheimer's disease: a systematic review and meta-analysis. Lancet Neurol 2016;15:673–684.
42. Vera JH, Guo Q, Cole JH, et al. Neuroinflammation in treated HIV-positive individuals: a TSPO PET study. Neurology 2016;86:1425–1432.
43. Roberts RO, Geda YE, Knopman DS, et al. Association of C-reactive protein with mild cognitive impairment. Alzheimers Dement 2009;5:398–405.
44. Yaffe K, Lindquist K, Penninx, et al. Inflammatory markers and cognition in well-functioning African-American and white elders. Neurology 2003;61:76–80.
45. Vlad SC, Miller DR, Kowall NW, Felson DT. Protective effects of NSAIDs on the development of Alzheimer disease. Neurology 2008;70:1672–1677.
46. Wang J, Tan L, Wang HF, et al. Anti-inflammatory drugs and risk of Alzheimer's Disease: an updated systematic review and meta-analysis. J Alzheimers Dis 2015;44:385–396.
47. Jaturapatporn D, Isaac MGEKN, McCleery J, Tabet N. Aspirin, steroidal and non-steroidal anti-inflammatory drugs for the treatment of Alzheimer's disease. Cochrane Database Syst Rev 2012;15:CD006378.
48. Braak H, Braak E. Neuropathological stageing of Alzheimer-related changes. Acta Neuropathol 1991;82:239–259.
49. Mattiace LA, Davies P, Yen SH, Dickson DW. Microglia in cerebellar plaques in Alzheimer's disease. Acta Neuropathol 1990;80:493–498.
50. Gui Y, Marks JD, Das S, Hyman BT, Serrano-Pozo A. Characterization of the 18 kDa translocator protein (TSPO) expression in post-mortem normal and Alzheimer's disease brains. Brain Pathol 2020;30:151–164.